Tertiary tectonic evolution of the external Southern Carpathians and the adjacent Moesian platform (Romania)

Matenco, L.; Bertotti, G.V.; Dinu, C.; Cloetingh, S.A.P.L.

published in
Tectonics
1997

DOI (link to publisher)
10.1029/97TC01238

document version
Publisher's PDF, also known as Version of record

TECTONICS, VOL. 16, NO. 6, PAGES 896-911, DECEMBER 1997

Tertiary tectonic evolution of the external South Carpathians and the adjacent Moesian platform (Romania)

L. Maţenco,[1] G. Bertotti,[2] C. Dinu,[1] and S. Cloetingh[2]

Abstract. Depth-interpreted seismic sections of the Getic Depression foredeep, paleostress indicator data and analysis of outcrop- to regional-scale structures are integrated to derive the tectonic evolution of the South Carpathians - Moesian platform area. Following Late Cretaceous and older orogenic phases, the South Carpathians - Moesian platform area underwent strike-slip deformation with NE-SW oriented compression and NW-SE tension. In Paleogene to Early Burdigalian times, tensional deformation is recorded which led to the opening of WSW-ENE to E-W trending extensional basins. In the Late Burdigalian, NE-SW oriented contraction took over causing the oblique inversion of preexisting extensional structures. During Sarmatian times, NW-SE and slightly younger N-S trending compression caused the activation of mainly NW-SE dextral strike-slip faults and, in the frontal areas, south directed thrusting. The NW-SE direction of extension determined for Paleogene to Early Burdigalian times is hardly compatible with presently accepted models of substantially continuous dextral wrenching between the Intra-Carpathians units to the north of the South Carpathians and the Moesian platform to the south. In contrast, we have demonstrated dextral transpressive to transtensional movements within an E-W trending corridor from the Late Burdigalian to Late Sarmatian which are compatible with available models.

1. Introduction

The Romanian segment of the Carpathians is a highly arcuate mountain belt formed during Alpine, roughly eastward movement of the Intra-Carpathians units and continental collision between the Eurasian and Apulian plates [*Săndulescu*, 1984; *Csontos*, 1995]. The Carpathians consist of an Alpine nappe pile of crystalline units and upper Paleozoic-Mesozoic sediments, with an uppermost Cretaceous to Tertiary sedimentary cover (Figure 1). The Alpine history of the Carpathians area is traditionally subdivided in a Triassic to Neocomian extensional stage followed by mainly contractional deformation lasting from Neocomian throughout Tertiary times [*Săndulescu*, 1988].

The South Carpathians represent an important segment of the belt and stretch from the orocline bending of western Romania - eastern Serbia in the west to the junction zone with the East Carpathians in the east. Following the mentioned tectonic scheme, deformation of the South Carpathians would be dominated by dextral wrenching between the Intra-Carpathians units in the north and the Moesian platform in the south. A number of studies have focused on the structure of the internal parts of the South Carpathians [e.g., *Murgoci*, 1905, 1912; *Streckeisen*, 1934; *Codarcea*, 1940; *Berza et al.*, 1983; *Balintoni et al.*, 1989; *Ratschbacher et al.*, 1993; *Berza*, 1994; *Linzer*, 1996]. Fewer papers have been published on the foredeep area [*Motaş*, 1983; *Ionescu*, 1994, *Dicea*, 1995]. The kinematic and dynamic relations between the South Carpathians fold-and-thrust belt and the adjacent foredeep basin have received very little attention also because of the lack of data from the transition zone between the orogenic belt and the undeformed foreland. This zone can play a key role in the integrated interpretation of the area. A well-constrained comprehension of the kinematics and deformation in the South Carpathians region is crucial for the understanding of the formation of Carpathians highly arcuate feature as a whole.

In this study, we document foredeep depth structures obtained from seismic and well interpretation in order to constrain the large-scale kinematic stages of the area located between the orogen in the north and the undeformed Moesian platform farther in the south. Outcrop- and regional-scale structural data from the external part of the South Carpathians are then presented, which allow for the determination of relevant features such as stress regime and transport directions. We devote particular attention to basin formation processes and their evolution through time.

2. Tectonostratigraphic Setting and Previous Interpretations

The 150-200 km wide area between the axial part of the South Carpathians and the undeformed part of the Moesian platform (Figure 1) is known as Getic Depression and accommodates more than 6 km of Upper Cretaceous to Tertiary sediments deposited in a polyphase tectonic regime.

The northern part of the area is occupied by the South Carpathians nappe pile. The following major nappes can be schematically recognized in the basement units from top to bottom: the Supra Getic nappe, between Dâmboviţa and Olt valleys, thrust over the Getic nappe during the Middle Cretaceous [*Săndulescu*, 1984, 1988]; the Getic nappe, between Olt and Olteţ valleys and, as remnants, at Vălari and between Motru and Danube valleys, thrust over the Severin nappe in the middle Cretaceous [*Codarcea*, 1940; *Săndulescu*, 1984, 1988; *Berza*, 1994]; and the Danubian "Autochthone" (as was previously defined in Romanian literature) thrust sheets outcropping between the Olteţ and Danube valleys, representing slices of European continental crust emplaced during Laramian contraction in association with thrusting of overlying Getic and Severin tectonic units [*Berza et al.*, 1983]. The South

[1] Faculty of Geology and Geophysics, Bucharest University, Bucharest.
[2] Faculty of Earth Sciences, Vrije Universiteit, Amsterdam.

Paper number 97TC01238.
0278-7407/97/97TC-01238$12.00

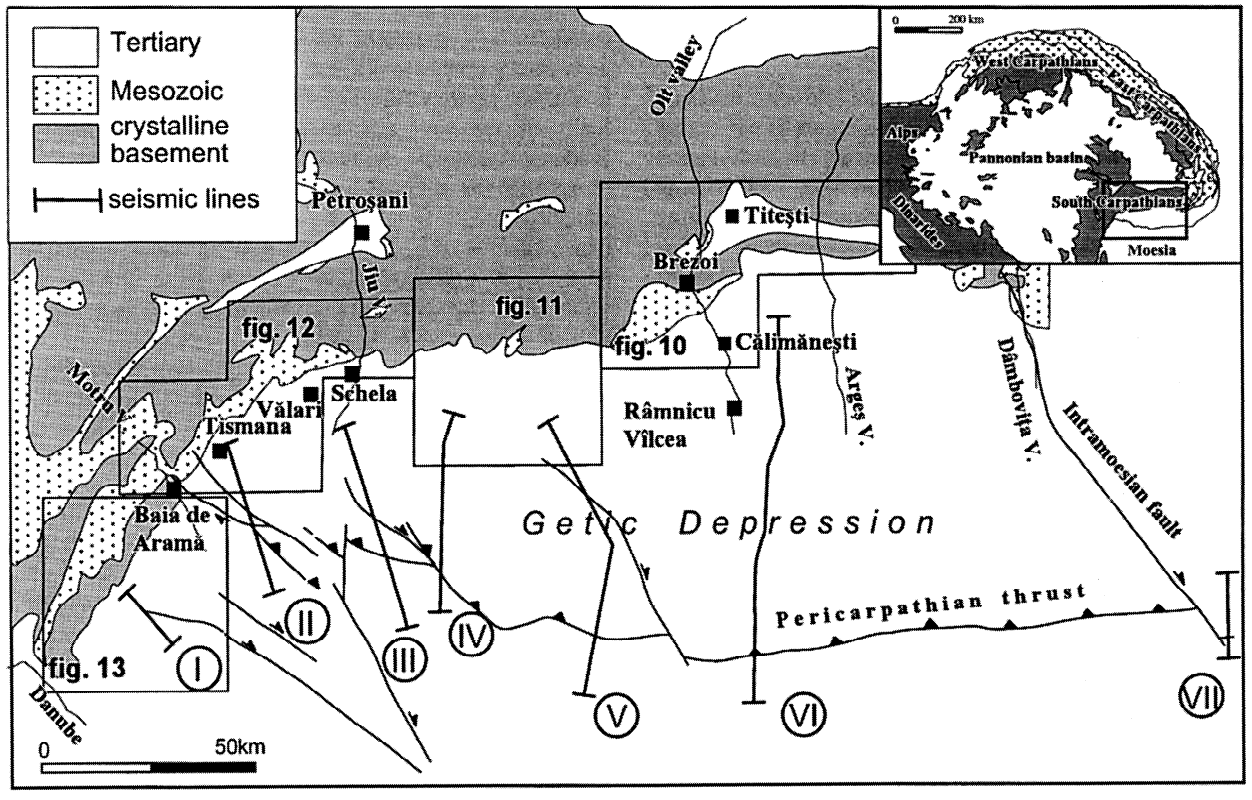

Figure 1. Location map of the South Carpathians external area. Thick lines denote seismic interpreted profiles in the foredeep zones. Boxes give the position of the geological/ structural maps discussed in detail.

Carpathians nappe pile is unconformably covered by more than 2 km of south dipping Upper Cretaceous to Paleogene sediments followed toward the south by progressively younger and flatter-lying deposits. Pliocene to Quaternary sediments form the undeformed cover of the Moesian platform in the southernmost parts of the considered area.

The sedimentation history of the Getic Depression can be schematically subdivided into three main stages: (1) from latest Cretaceous to Paleogene, (2) from Early Miocene (Early Burdigalian) to Late Miocene (Late Sarmatian), and, (3) from the latest Sarmatian to Late Pliocene (Late Romanian).

During the latest Cretaceous to Paleogene, a thick, coarse-grained clastic succession was deposited on the inner basement formed by the Getic, Severin, and the Danubian nappes [*Jipa*, 1980, 1982, 1984]. Traditional interpretations [*Săndulescu*, 1984, 1988; *Ştefănescu and Polonic*, 1993] consider this succession as a molasse of the Laramian phase (Dacidic Molasse) but fail in providing a mechanism for the substantial subsidence required by the thickness of the Upper Cretaceous to Paleogene succession. According to more recent interpretations [*Ratschbacher et al.*, 1993], the Moesian platform acted during Alpine orogeny as a rigid "corner" imposing Late Cretaceous to Paleogene dextral wrenching in the South Carpathians and causing E-W compression and subsidence in its northern part.

In Early to Late Miocene times, the prestructured Carpathians nappe pile was thrust toward the south, flexing the northern part of the Moesian platform and allowing for the deposition of a southward thinning clastic wedge. The internal part of the wedge, where sediments are more than 3 km thick, was progressively involved in shortening and presently forms a well developed fold-and-thrust belt. The trace at the surface of the outermost thrust is named Peri-Carpathians line in the Romanian literature (Figure 1). Toward the west, the frontal thrust is transferred into the strike-slip system formed by the Cerna, Timok and related faults and does not follow the western bending zone of the Southern Carpathians. According to *Săndulescu* [1984] and *Royden* [1988], the Getic Depression is continuous toward the east with the most external nappe of the East Carpathians (Subcarpathian nappe). Both the width of the wedge and the amount of southward thrusting decrease from east to west; no explanation has been proposed for these lateral changes. Reverse faulting in the South Carpathians and thrusting in the internal foredeep areas were probably contemporaneous with large-scale strike-slip movements between Transylvania and Moesia and with thrusting in the Eastern Carpathians. Quantitative kinematic relations between these various processes still have to be worked out.

Upper Sarmatian (Late Miocene in Paratethys timescale) sediments transgressively cover the tectonic edifice and mark the end of thrusting and foredeep basin evolution. Upper Sarmatian to Pliocene (Meotian, Pontian, Dacian, and Romanian in the Paratethys timescale) sediments reach their maximum thicknesses along the Peri-Carpathians line but are found from central Moesia in the south to the Carpathians in the north. Here the present-day outcrop limit is of erosive nature, and therefore it is unknown how far to north the Upper Sarmatian sediments

extended. Upper Romanian deposits in the eastern part of the Getic Depression show small-scale deformation and local thrusting.

Structures and small sedimentary basins closely associated with the development of the Getic Depression are found also in more internal areas (so-called "intramontane" basins). In the Brezoi - Titcşti Basin (Figure 1) the sedimentary succession is formed by Upper Cretaceous conglomerates and marls sealing the Laramian Upper Getic nappe contact [*Hann and Szasz,* 1984; *Hann,* 1995] and by Paleocene to Lower Miocene siltstones to conglomerates [*Szasz*, 1975; *Ştefănescu et al.*, 1986, 1988]. Farther to the west, in the Tismana - Schela region (Figure 1), the Lower Jurassic to Senonian sedimentary cover of the crystalline basement [*Marinescu et al.*, 1989] has been deformed during the Cretaceous but also shows Tertiary tectonic structures which can be correlated with those of the Getic Depression.

One of the controversial topics is wether deformation in the external South Carpathians and in the adjacent Getic Depression can be considered as plane-strain N-S contraction or if dextral transpressive movements in the zone between the South Carpathians nappe pile and the Moesian Platform are of substantial importance. According to *Săndulescu* [1984, 1988], the external South Carpathians became active only during the Late Miocene, when the strike-slip displacement along the northern prolongation of the Timok and related faults in the inner belt (e.g., Cerna fault) was gradually transformed into thrusting. *Royden* [1988] suggested that the shortening within the southern part of the outer Carpathians belt was kinematically linked to right-lateral slip south of the Transylvania Basin; to the west, deformation was transferred into the Timok and related dextral strike-slip faults (Cerna) at the Miocene level (starting Late Miocene-Early Pliocene). *Ratschbacher et al.* [1993] pointed out that Tertiary convergence along the southwestern margin of the Moesian platform can be classified as dextral oblique and decomposed into a strike-slip component along the plate boundary (inner South Carpathians) and a normal component taken up by the transpressional thrust belt of the Getic Depression.

3. Foredeep Data Analysis

A large number of seismic profiles across the Getic Depression has been shot in the last decades leading to the recognition of important subsurface structures which formed in Tertiary and Early Quaternary times in response to South Carpathians convergence and following events. The kinematics of these structures are, however, complex and change both laterally and temporally. We base our description on published and unpublished geological interpretations of roughly N-S trending seismic profiles. For the sake of simplicity, we will subdivide the area into four domains from west to east (Figures 1 and 2): (1) between the Danube and Motru valleys, (2) between the Motru and Olteţ valleys, (3) between the Olteţ and Olt valleys, and (4) between the Olt valley and Dâmboviţa valleys.

3.1. Danube - Motru Valleys Sector

A characteristic feature of this area is the presence of large, mainly NE-SW striking normal faults which displace Cretaceous to Paleogene beds (Figure 3). The first formations for which we can recognize fault-controlled thickness changes are of Paleogene age. Extension continued during the Early Miocene and ended probably in the Early Burdigalian. Poorly dated lower to middle Burdigalian coarse-grained clastics onlap the normal fault escarpments and have therefore a postextensional character. The faults are, in general, parallel to the curved trend of the inner basement and are found as far to the NE as the Olt valley (Figure 2). Lower to Middle Burdigalian sediments reach their maximal thicknesses of 2000 m along a ENE-WSW elongated depression (Zegujani Depression) and are found as far south as the Bulbuceni area (Burdigalian southern transgression limit of the petroleum industry).

The entire extensional system is partly inverted to high-angle reverse faults which seem to be interconnected at depth, with strata rotations on these reverse faults. A strike-slip character can be postulated on the basis of deformation geometry. The faults truncate the sedimentary wedge up to Lower Sarmatian and are covered by Upper Sarmatian deposits. These features demonstrate a Sarmatian transpressional tectonic regime, characterized by positive flower structures (Figure 3).

3.2. Motru - Olteţ Valleys Sector

Evidence for extension prior to Late Burdigalian is found farther to the east in the area between the Motru and Jiu valleys (Figure 4 sections II, III, and IV). Extensional faults, as seen in unpublished seismic lines, have a ENE-WSW direction and displacements smaller than those observed in the west. Reverse and thrust faults appear which will become more important in the eastern zones. Inversion of normal faults and activation of new thrust faults frequently forming faultpropagation folds also document contractional tectonics. The over 2000 m thick basin fill prior to Upper Burdigalian, has been scooped out and transported toward the SW on the Moesian platform devoid of Paleogene to Lower Miocene formations. The direction of the main thrust faults in the region is NW-SE (Figure 2) and therefore strongly oblique with respect to the older normal faults. The southward thinning wedge shape of the Burdigalian sediments is partly caused by the previous extensional structures, but it is also the result of thrust-related thickening and flexural subsidence. Most of the thrust faults are sealed by Badenian deposits thus marking the end of shortening.

Fault activity resumed in Sarmatian times with the development of medium-angle thrust faults with northward dip which are probably connected in depth with northward dipping vertical or subvertical normal faults (Figure 4). More importantly, strike-slip faults developed and formed transpressional flower structures. During their growth, they influenced sedimentation in the adjacent areas. The faults truncate Upper Sarmatian to Lower Meotian deposits. Sarmatian deposits onlapping both sides of flower structures and thickness variations demonstrate the Sarmatian age of strike-slip deformation. In interpreted seismic sections, the structures appear tilted toward the foreland because of the strong transpressional character and the related south vergent ramping on the Moesian platform. In map view, the faults trend WNW-ESE in the north and assume a more NW-SE position moving southward. Strike-slip duplexes are common along the main faults, forming the oil structures lineaments at Ţicleni, Bulbuceni, and Bustuchini (Figures 1 and 2) as well as in other areas.

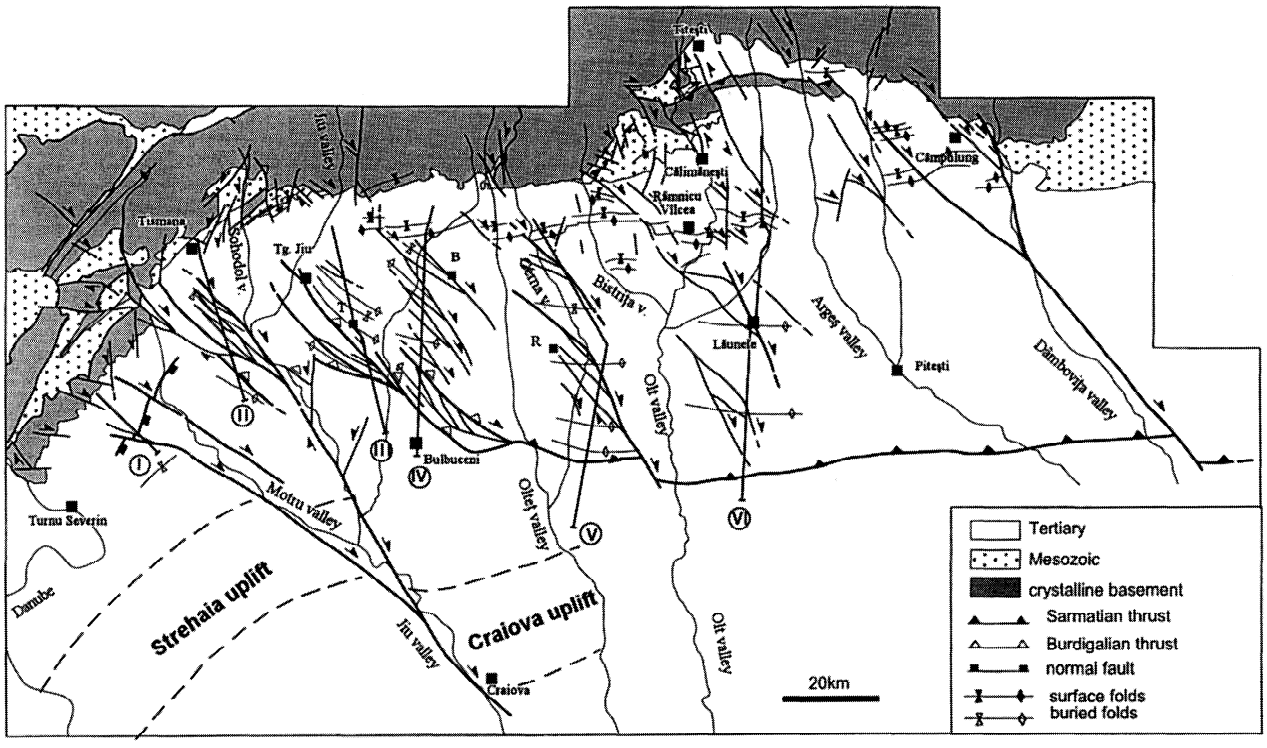

Figure 2. Structural map of the area between the external South Carpathians and the northern part of the Moesian platform. Structures in the Getic Depression are presently buried beneath younger sediments. Dashed lines indicate supposed fault traces. Smaller faults in the Moesian platform and faults with unknown sense of movement are not included.
Note the prolongation of dextral faults from basement into the transpressional structures in the foredeep, later sinistral faults displacing these structures, the supposed crustal fault between the Strehaia and Craiova uplifts, and the Intramoesian fault (extreme east) prolonging toward the inner South Carpathians in a horsetail structure. Abbreviations as follows; T, Ţicleni; B, Bustuchini; R, Românești.

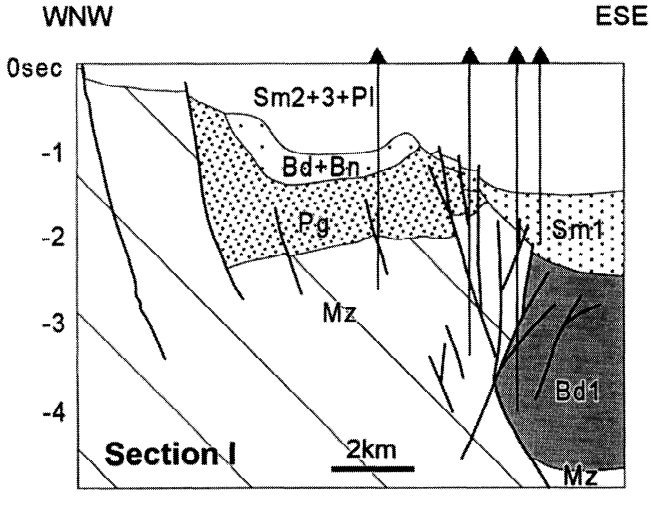

Figure 3. Geological interpretation of seismic profile I (after *T. Răbăgia,* unpublished data, 1995). Depth axis in two-way travel time. Notice the presence of major normal faults, reactivated by a positive flower structure. Position of the profile is indicated in Figures 1 and 2. Abbreviations as follows; Mz, Mesozoic; Pg, Paleogene; Bd1, Burdigalian; Bd+Bn, Burdigalian + Badenian; Sm1, Lower Sarmatian; Sm_{2+3} + Pl, Middle-Upper Sarmatian to Pliocene.

3.3. Olteţ - Olt Valleys Sector

Interpreted seismic sections in this area (Figure 5) also provide evidence for Burdigalian tectonics. A number of medium- to high-angle reverse faults are observed reaching into the Burdigalian beds. They typically merge at depth with high-angle, hinterland-dipping normal faults or with hinterland-vergent thrust faults. Laterally, inversion of older normal faults, is common. Burdigalian deposits have a pronounced wedge geometry which is compatible with the larger amount of thrusting which affected this section.

The dominant structures found in the area are related to Sarmatian deformations. Deposits prior to Lower Sarmatian, were thrust over Mesozoic and, farther to the south, over Middle to Upper Sarmatian sediments of the Moesian platform. A detail of the frontal thrust along profile V is shown in Figure 6. Notice the pre-Lower Sarmatian thrusting, the development of secondary Upper Burdigalian - Badenian piggyback basin tilted by later Sarmatian deformations, and the Pliocene sealing of the thrust system. The strike of the frontal thrust is E-W (Figure 2), suggesting a N-S transport direction. Important NW-SE trending strike-slip to transpressional deformations zones formed; in some cases, such as in the western areas, a reactivation of Burdigalian structures can be demonstrated. Two such NW-SE trending lineaments can be defined in this area and are visible in

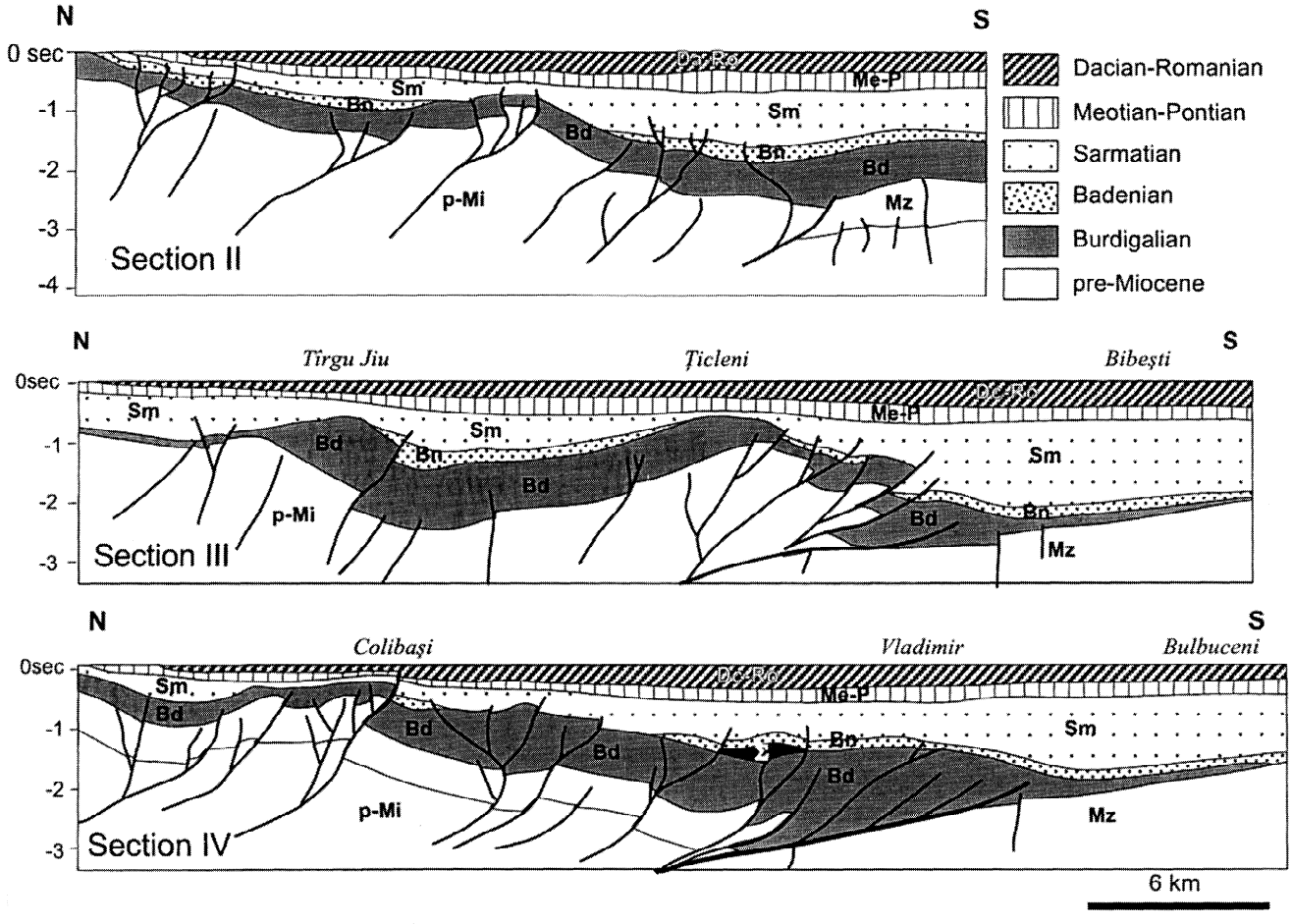

Figure 4. Geological interpretation of seismic profiles II, III, and IV. Positions of profiles are indicated in Figures 1 and 2. S in profile IV denotes salt bodies.

the interpreted seismic sections: one close to the northern basin border and a more important one in median position, with significant uplift, in the Romănești - Zărnești area (Figures 5 and 6). The latter forms an important flower structure tilted toward the foreland by dextral transpression and advancement over the platform. This strike-slip structure separates two distinct depocenters at Upper Sarmatian - Lower Pliocene level suggesting that its activity continued until Early Pliocene times.

3.4. Olt - Dâmboviţa Valleys Sector

The easternmost area, between the Olt and Dâmboviţa valleys is characterized by dramatic increase in width of the orogenic wedge which reaches roughly 80 km (Figure 7). The main frontal thrust consistently preserves a E-W direction (Figure 2) and is accompanied by a large number of smaller, reverse faults (Figure 7). Similarly to the previous section, Burdigalian and older deposits are thrust on the Mesozoic to

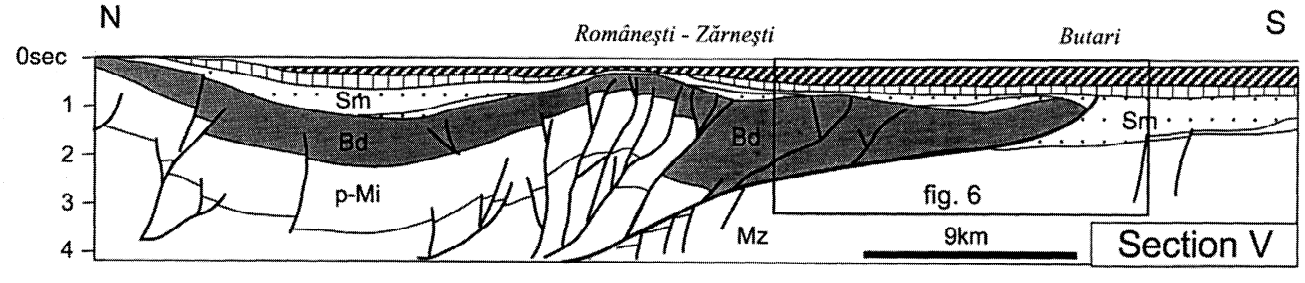

Figure 5. Geological interpretation of seismic profile V. The position of the profile is given in Figures 1 and 2. Legend is as in Figure 4. The box gives the location of seismic profile in Figure 6.

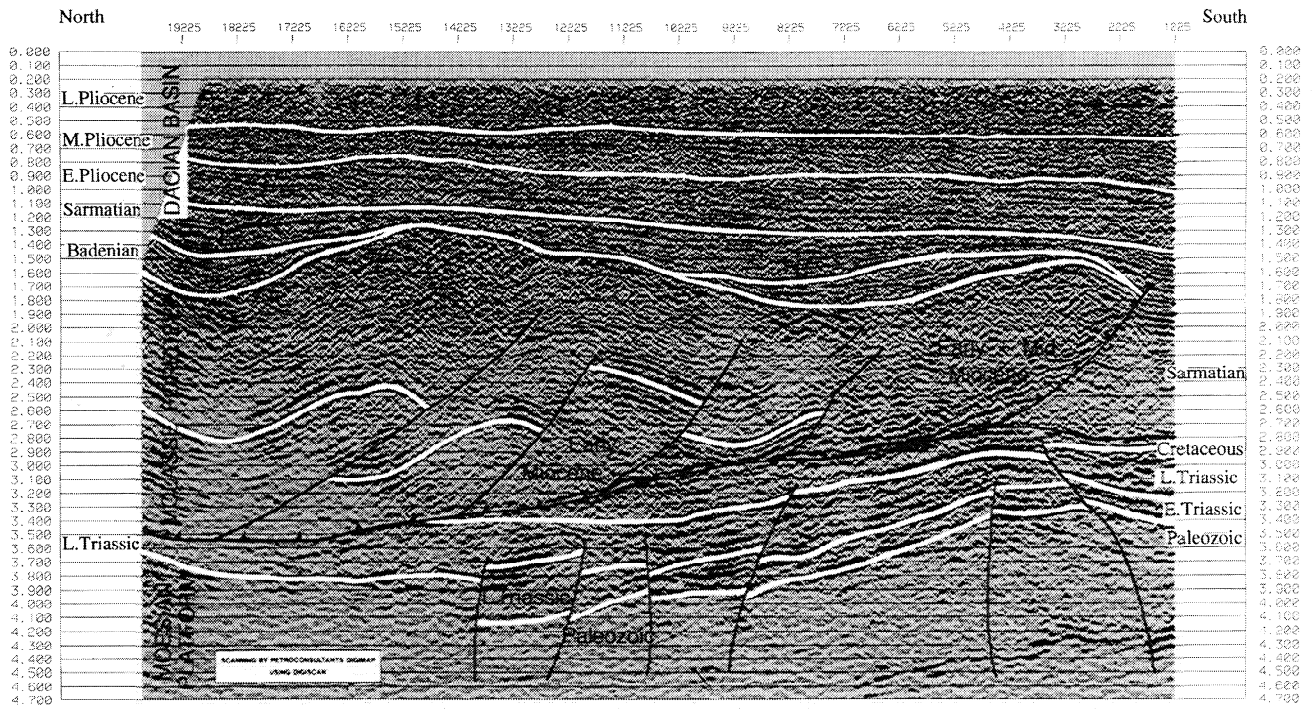

Figure 6. Seismic line showing the detailed structure of the frontal thrust between Jiu and Olt valleys [after Ionescu, 1994] roughly corresponding to section V, Figure 5. Note overthrusting of Lower Miocene sediments over the Sarmatian deposits, and the development of Badenian piggyback basins which have been tilted by later Sarmatian deformation.

Middle Sarmatian sediments of the Moesian platform. The Burdigalian-Lower Sarmatian deposits are clearly thickened in correspondence with the main thrust.

Strike-slip to transpressional fault zones are common and have a NW-SE direction (Figures 2 and 7). They often form uplifted structures as in the Săpunari-Lăunele area (Figure 1) where Paleogene deposits define two distinct Upper Sarmatian - Lower Pliocene sedimentation basins overlain by Lower Meotian sediments. The uplifted area is delimited by high-angle reverse faults toward foreland and normal faults toward hinterland. While the depth prolongation of these faults is difficult to trace, we propose that the Săpunari-Launele uplift represents a transpressional structure slightly rotated toward the foreland. While most of deformation ended in Late Sarmatian times, local thrusting in the nappe front, backthrusting and local folding mainly concentrated near the northern border of the basin and persisted through Pliocene times. The overall shortening accommodated in the thrust sheet overlying the frontal thrust has been estimated at more than 30 km [*Morariu et al.*, 1992].

Farther to the east, a major NW-SE trending crustal fault, the Intramoesian fault, separates the Getic Depression from the East Carpathians foreland (Figures 1 and 2). The fault, defined as an older crustal fracture, shows important Neogene reactivation [*Săndulescu*, 1988]. Significant dextral movement is demonstrated by interpreted seismic profiles and is compatible with other NW-SE trending strike-slip zones described in previous sections. The Intramoesian fault might have played an important role in the southeastward movement of the Carpathians bend zone. East of the Intramoesian fault, Pliocene deformation is also observed (Figure 7) and becomes more and more intense moving eastward toward the bend zone [e.g., *Hyppolite and Săndulescu*, 1996]. Pliocene contraction also played a relevant role in the development of salt diapirs in the frontal part of buried thrusts (Figure 8).

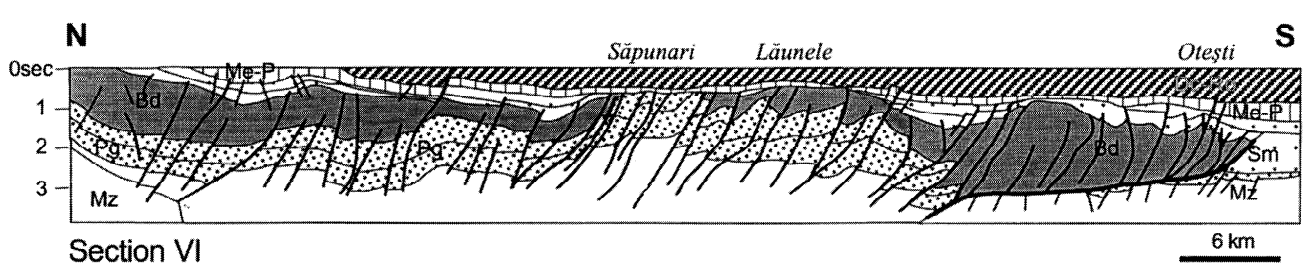

Figure 7. Geological interpretation of seismic profile VI. The position of the profile is given in Figures 1 and 2. Legend is as in Figure 4.

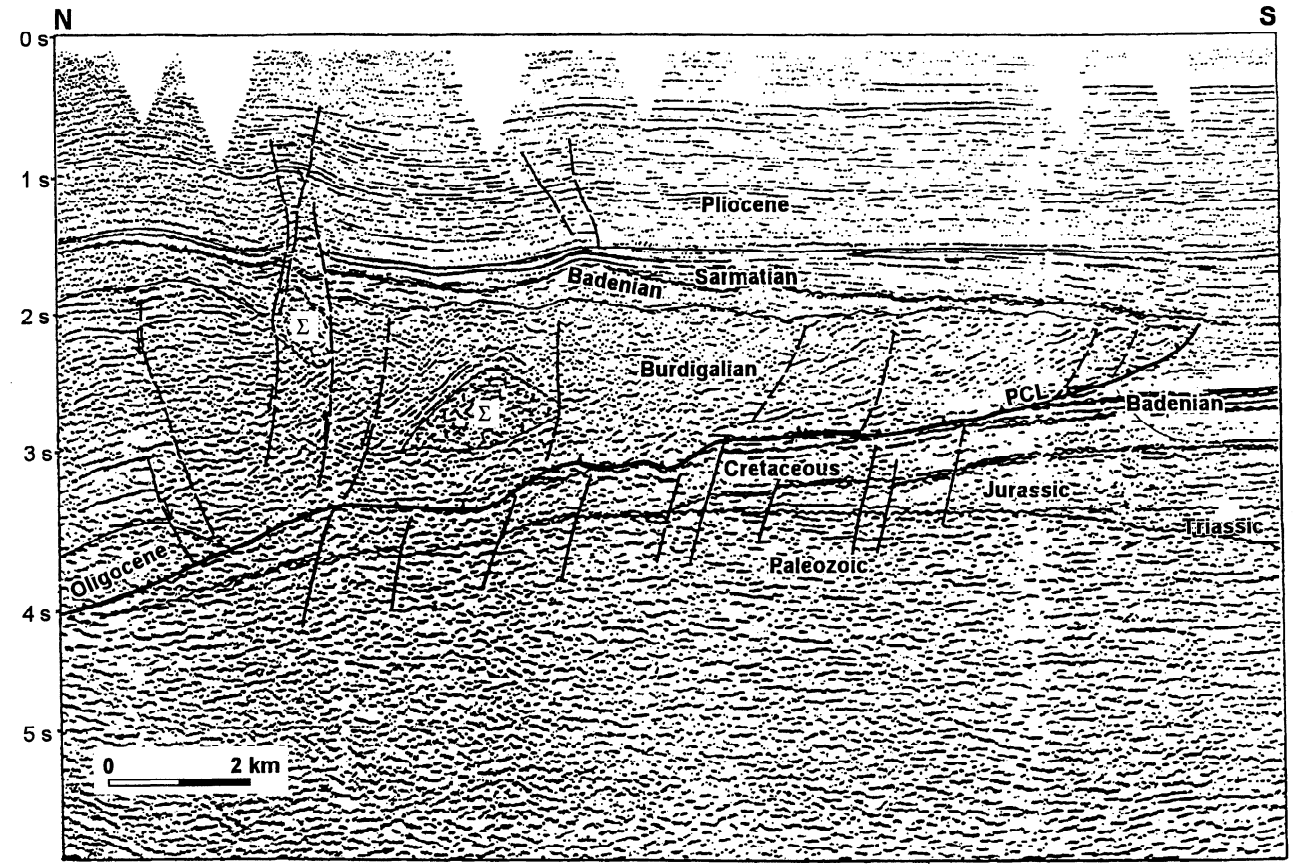

Figure 8. Interpreted seismic profile (VII) east of the Intramoesian fault [after *Dicea*, 1995]. Note the same characteristics of the thrusts as in the foreland area of Getic Depression in the eastern part, and the local Burdigalian salt structures. The frontal thrust is more advanced toward the south than immediately west of the Intramoesian fault. Position of the profile in Figures 1 and 2.

4. Field Analysis

Fieldwork was carried out in a broad area of the external South Carpathians and adjacent foreland from the Danube valley in the west to the Intramoesian Fault in the east with the main goal of providing farther geometrical constraints for the evolutionary stages detected in the foredeep subsurface. The structural analysis was carried out on Cretaceous to Sarmatian foredeep sediments outcropping along the southern border of the South Carpathians, on the neighboring basement units, and in intramontane depressions (Figure 1). Toward the south, a thick pile of Plio-Pleistocene sediments covers older successions and structures and provided no information.

4.1. Data and Methods

We have analyzed structures such as striated faults, folds, tension joints, fault-related folds and regional-scale faults for a total of 105 stations. For regional correlations, we have used the field data obtained by *Ratschbacher et al.* [1993] in the "intramontane" (Haţeg, Petroşani, and Vidra) basins, regional syntheses by *Berza et al.* [1994], *Neubauer et al.* [1994], and also geologic maps published by the Geological Institute of Romania (IGR), scale 1:50,000.

Regional paleostress directions were reconstructed using the fault slip data sets collected on 70 stations along the belt (Figures 9 to 13). Most of the data sets (57 stations) were analyzed using the *Angelier* [1984, 1989] inverse method (marked "inverse" on Table 1). The basic principle of the method is to obtain the best possible fit between the observed fault-slip and the calculated theoretical shear stress on these faults generated by the stress tensor. This analysis allows for the definition of the orientation of principal stress tensors ($\sigma_1 \geq \sigma_2 \geq \sigma_3$) and the ratio R between stress magnitudes ($R= (\sigma_2-\sigma_3)/(\sigma_1-\sigma_3)$) for a single deformation period. We used the TENSOR program kindly provided by D. Delvaux. This method could be applied where a large number of faults/stages of deformation was available. Conjugate faults were used in stations with few faults. The stress axes directions in these cases are marked "PT" in Table 1. Sets of tension joints and folds axes were measured in few stations. A first separation of faults was carried out in the field based on timing structures. Data processing also allowed for farther separation of fault sets. Relative timing relationships between the various tensors were determined on the basis of field evidence such as superposition of striations, on the basis of the age of the deformed sediments, and, more importantly, by correlating the tensors with large structures visible in seismic lines.

Table 1. Resulted Paleostress Tensors

Station	Latitude, deg, min, s	Longitude deg, min, s	σ_1	σ_2	σ_3	Method	Rock Age - Lithology
BR2 - DEX1	45 20 16	24 16 14	124/12	20/49	223/38	inverse	Upper Cretaceous - conglomerate
BR4 - TR	45 19 42	24 16 53	76/61	194/15	291/24	inverse	basement gneiss
BR4 - TR	45 18 58	24 17 16	230/11	79/60	320/02	PT	basement gneiss
BR51 - TR	45 21 09	24 12 51	188/52	72/18	330/31	inverse	basement gneiss
BR52 - DEX1	45 20 35	24 12 53	310/29	190/42	62/34	inverse	Upper Cretaceous sandy marl
BR53 - DEX1	45 20 04	24 14 59	106/71	304/18	212/06	inverse	basement gneiss
BR55 - DEX2	45 27 13	24 21 51	351/05	88/52	257/37	inverse	Paleocene-Ypresian conglomerate
BR56 - DEX1	45 24 39	24 21 53	308/10	179/70	40/10	inverse	Eocene marls, sandstone
BR58 - TR	45 21 55	24 22 23	240/25	75/64	333/06	PT	Eocene marls, sandstone
BR58 - DEX1	45 22 08	24 22 18	303/07	171/80	34/07	inverse	Eocene marls, sandstone
BR59 - TR	45 23 23	24 18 14	272/09	47/77	181/09	inverse	basement paragneiss
BR59 - DEX1	45 23 23	24 18 14	152/02	56/71	243/19	inverse	basement paragneiss
BR60 - TR	45 21 32	24 17 53	43/11	192/78	312/06	inverse	Upper Cretaceous conglomerate
BR60 - DEX1	45 21 32	24 17 53	308/01	146/89	38/01	inverse	Upper Cretaceous conglomerate
BR61 - TR	45 18 23	24 17 16	231/02	131/78	321/12	inverse	basement paragneiss
BR61 - DEX1	45 18 23	24 17 16	127/15	328/74	218/06	inverse	basement paragneiss
BR62 - DEX1	45 17 28	24 17 51	159/02	54/81	249/08	inverse	Upper Cretaceous sandstone
BR62 - EX	45 17 28	24 17 51	195/60	316/17	54/24	inverse	Upper Cretaceous sandstone
BR63 - DEX1	45 17 26	24 18 02	315/18	109/70	222/08	inverse	Upper Cretaceous sandstones, silt
BR63 - EX	45 17 26	24 18 02	287/66	111/24	021/21	inverse	basement paragneiss
BR64 - EX	45 17 06	24 18 30	42/73	155/07	247/15	inverse	basement gneiss
BR64 - DEX2	45 17 06	24 18 30	176/05	274/57	82/32	inverse	basement gneiss
BR65 - DEX2	45 15 55	24 20 39	13/12	184/78	283/02	PT	Eocene conglomerate
BR66 - EX	45 16 00	24 19 32	20/61	261/15	165/24	inverse	Upper Cretaceous sandstone, shale
BR68 - EX	45 12 00	24 03 28	92/37	301/49	193/15	inverse	Jurassic limestone
BR68 - DEX1	45 12 00	24 03 28	120/18	27/09	272/70	inverse	Jurassic limestone
BR69 - DEX1	45 11 57	24 03 58	103/28	294/61	196/05	inverse	Jurassic limestone
BR70 - CP	45 11 28	24 02 30	240/00	330/22	150/68	inverse	Jurassic limestone
BR71 - TR	45 16 32	24 07 53	215/11	109/55	312/33	PT	basement gneiss
BR71 - DEX1	45 16 32	24 07 53	113/23	302/67	204/03	inverse	Jurassic limestone
BR72 - DEX2	45 12 36	24 13 55	346/10	241/58	82/30	inverse	Eocene conglomerate sandstone
BR72 - EX	45 12 36	24 13 55	315/63	113/25	208/09	inverse	Eocene conglomerate sandstone
BR73 - DEX1	45 12 06	24 11 09	327/38	145/52	236/01	inverse	Upper Cretaceous sandstone
GTE1 - TR	45 22 13	24 36 55	79/52	238/36	336/11	inverse	basement gneiss
GTE2 - DEX2	45 24 39	24 37 53	171/28	274/22	35/53	inverse	basement gneiss
GTE5 - DEX2	45 20 50	24 40 00	196/21	43/67	290/09	PT	basement paragneiss
GTE6 - TR	45 21 19	24 43 53	227/17	53/73	318/02	PT	basement paragneiss
GTE6 - CP	45 21 40	24 43 28	223/06	133/04	9/83	inverse	basement paragneiss
GTE6 - EX	45 21 40	24 43 28	353/75	144/13	236/07	inverse	basement paragneiss
GTE7 - DEX2	45 20 05	24 44 28	172/15	75/25	290/61	inverse	Paleocene-Eocene conglomerate
GTE8 - TR	44 25 16	24 48 55	229/15	95/69	323/15	inverse	basement paragneiss
GTE9 - CP	45 21 40	24 30 21	224/07	322/48	128/41	inverse	basement gneiss
GTE9 - DEX2	45 22 21	24 30 25	185/27	23/62	279/08	PT	basement gneiss
GTE10 - EX	45 25 42	24 29 05	171/85	11/05	281/02	inverse	basement granite
GTE11 - CP	45 18 26	25 00 18	90/02	360/25	185/65	inverse	Eocene sandstone
GTE12 - CP	45 17 47	25 08 23	95/03	5/01	252/87	inverse	Jurassic limestone
GTW3 - CP	45 00 17	22 51 16	245/14	141/44	348/43	inverse	Barremian-Aptian limestone
GTW4 - DEX1	45 05 26	22 55 21	140/22	330/68	231/03	inverse	basement granite
GTW4 - EX	45 06 02	22 55 30	8/78	109/02	200/12	PT	basement granite
GTW5 - CP	45 05 47	22 58 35	235/36	328/03	62/54	inverse	Barremian-Aptian limestone
GTW5 - DEX2	45 05 47	22 58 35	180/08	279/48	83/40	inverse	Barremian-Aptian limestone
GTW6 - CP	45 06 58	23 00 30	51/09	144/20	297/68	inverse	basement paragniess
GTW6 - DEX1	45 06 58	23 00 30	126/14	300/76	36/01	inverse	basement paragneiss
GTW7 - CP	45 07 34	23 02 14	100/21	355/36	215/47	inverse	Upper Jurassic limestone
GTW7 - DEX2	45 07 34	23 02 14	163/27	23/56	262/19	inverse	Upper Jurassic limestone
GTW8 - DEX2	45 06 36	23 02 32	177/06	87/03	327/84	inverse	Barremian-Aptian limestone
GTW8 - EX	45 06 36	23 02 32	275/54	99/36	8/02	inverse	Barremian-Aptian limestone
GTW9 - DEX1	45 11 16	23 08 00	330/04	213/81	61/08	inverse	basement granite
GTW10 - EX	45 10 38	23 08 05	298/77	49/05	140/12	PT	Upper Jurassic-Aptian limestone
GTW11 - CP	45 09 28	23 07 53	89/10	358/05	245/79	inverse	Barremian-Aptian limestone
GTW13 - DEX2	45 08 23	23 08 23	166/24	70/13	313/62	inverse	Barremian-Aptian limestone

Table 1. (continued).

Station	Latitude, deg, min, s	Longitude deg, min, s	σ_1	σ_2	σ_3	Method	Rock Age - Lithology
GTW14 - TR	45 09 29	23 11 35	59/51	209/35	310/15	inverse	Upper Jurassic-Aptian limestone
GTW14 - CP	45 09 29	23 11 35	235/04	327/25	136/65	inverse	Upper Jurassic-Aptian limestone
GTW14 - DEX1	45 09 29	23 11 35	335/17	136/72	243/06	PT	Upper Jurassic-Aptian limestone
GTW14 - EX	45 09 29	23 11 35	253/77	73/13	163/00	PT	Upper Jurassic-Aptian limestone
GTW15 - DEX2	45 11 32	23 18 00	24/06	178/66	275/03	PT	Lower Jurassic metapelite
GTW16 - DEX1	45 11 10	23 21 51	163/25	36/52	266/26	inverse	basement granite
GTW16 - DEX2	45 11 10	23 21 51	180/19	273/09	28/69	inverse	basement granite
GTW17 - CP	45 12 44	24 00 21	230/28	339/32	107/45	inverse	basement paragneiss
GTW17 - DEX2	45 12 44	24 00 21	28/28	174/57	290/15	inverse	basement paragneiss
GTW18 - DEX1	45 12 10	23 54 41	310/11	210/42	52/46	inverse	basement paragneiss
GTW18 - DEX2	45 12 10	23 54 41	5/20	202/69	97/06	inverse	basement paragneiss
GTW19 - CP	45 12 03	23 51 37	25/10	117/11	254/75	inverse	basement paragneiss
GTW19 - TR	45 12 03	23 51 37	80/07	186/67	347/22	inverse	basement paragneiss
GTW20 - DEX1	45 14 26	23 49 09	166/13	266/35	58/52	inverse	Jurassic limestone
GTW20 - DEX2	45 14 26	23 49 09	205/37	22/53	114/01	inverse	basement paragniess
GTW21 - DEX1	45 13 34	23 44 18	310/06	42/21	205/69	inverse	Tithonian-Neocomian limestone
GTW21 - DEX2	45 13 34	23 44 18	178/25	48/54	280/24	inverse	Tithonian-Neocomian limestone
GTW22a DEX1	45 12 00	23 34 41	300/25	104/64	207/06	PT	basement granite
GTW22b DEX1	45 11 41	23 31 37	322/05	73/76	231/13	PT	basement migmatite
GTW22 - DEX1	45 12 55	23 40 28	151/25	47/28	277/51	inverse	basement granite
GTW22 - DEX2	45 12 55	23 40 28	221/72	4/15	97/10	inverse	basement granite
GTW23 - DEX1	45 04 10	22 53 30	323/16	232/03	129/73	inverse	basement granite
GTW24 - DEX1	44 55 28	22 46 42	305/16	173/67	40/16	inverse	basement amphybolite
GTW24 - TR	44 55 28	22 46 42	213/01	305/60	122/30	inverse	basement amphybolite
GTW25 - DEX1	44 51 47	22 46 00	330/06	194/82	61/06	inverse	Jurassic limestone
GTW25 - EX	44 52 49	22 47 37	357/62	206/25	110/12	PT	Jurassic limestone
GTW26 - DEX1	44 40 26	22 32 55	315/00	56/85	225/05	inverse	basement micaschyst
GTW26 - EX	44 40 44	22 31 51	4/84	205/05	115/02	PT	basement gneiss
GTW27 - DEX1	44 45 18	22 37 05	285/37	83/51	187/11	inverse	basement paragneiss
GTW27 - EX	44 46 06	22 36 46	162/74	27/11	295/11	PT	basement micashist
GTW28 - DEX1	44 48 44	22 40 51	332/11	99/72	239/14	PT	basement gneiss
GTW28 - EX	44 48 06	22 41 00	335/90	183/00	93/00	inverse	basement gniess
GTW29 - DEX2	45 11 57	23 46 46	6/17	134/64	270/20	inverse	Jurassic limestone

BR, GTE, and GTW are abbreviations for Brezoi-Titeşti, Getic East, and Getic West, respectively. TR, first set; EX second set; CP third set; DEX1 first subset of the fourth set, and DEX2 second subset of the fourth set. Inverse represents fault data analyzed with *Angelier*'s [1984, 1989] shear stress method, PT represents the conjugate faults method.

4.2. Results of Field Analysis.

Incompatible slip sense in paleostress data and evidence of reactivated structures support the existence of a polyphase history with different deformation geometries at different time intervals. This is also suggested by the different directions of principal tensors obtained through the processing of fault slip data. We present evidence for four major deformation geometries during the Tertiary in a old-to-young succession.

4.2.1. Strike slip with NE-SW compression. The first data set ("TR" set of Table 1) is characterized by a NE-SW σ_1 =230±20° (±20° is the average deviation from the measured stress direction) of the maximum horizontal compression direction and subhorizontal, NW-SE tension (σ_3 =320±20°) (Figures 9 and 10). Half of the stations for which a R value could be determined show a pure strike-slip character; the others are closer to transtensional.

Large-scale structures related to this stage are difficult to detect because of the limited amount of data and of later reactivations. However, a number of faults in Brezoi - Titeşti Basin and Călimăneşti - Buciumeni area can be included in this deformation stage (Figure 10). They are roughly N-S oriented

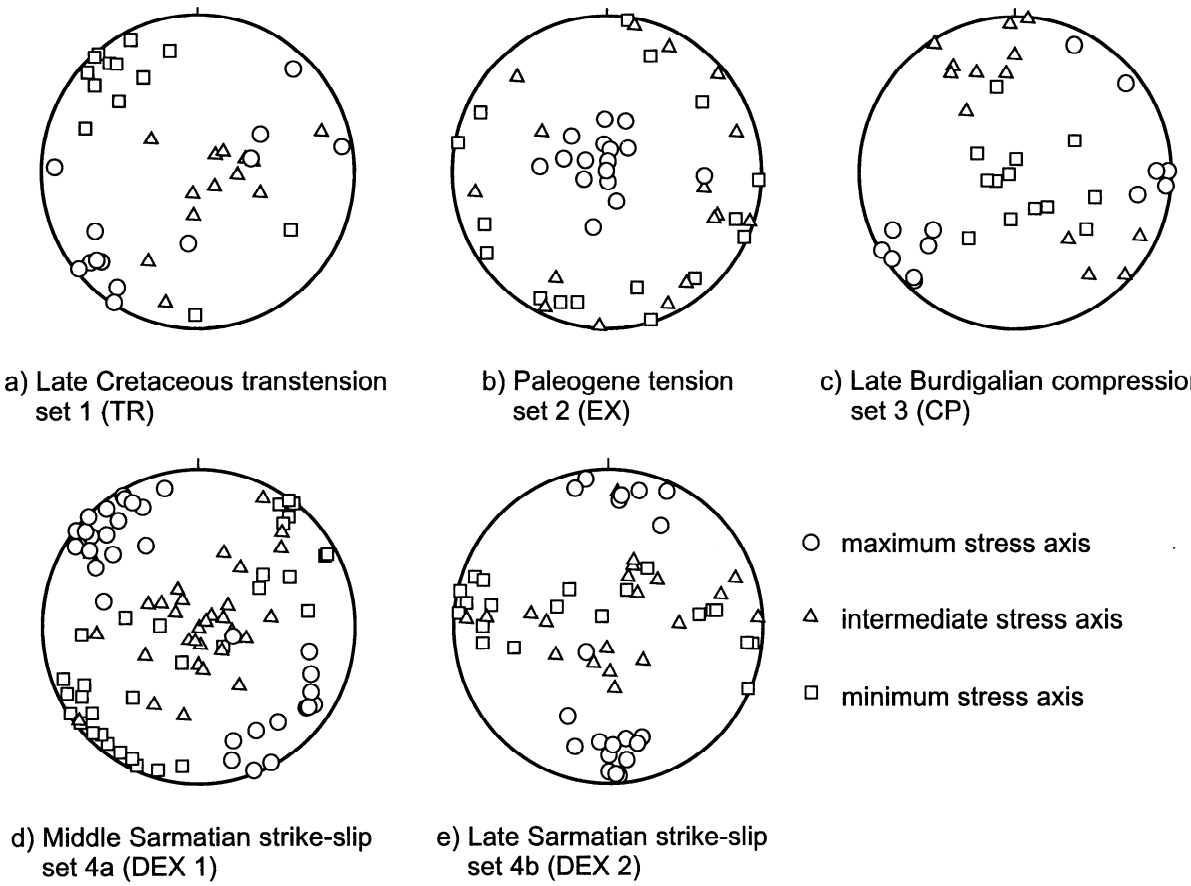

Figure 9. Lower hemisphere, equal area projection for principal stress directions obtained for each deformation phase: (a) Late Cretaceous transtension, (b) Paleogene (?)-Early Burdigalian tension, (c) Late Burdiglian compression, (d) Middle Sarmatian dextral shearing, (e) Late Sarmatian sinistral shearing and dextral reactivation.

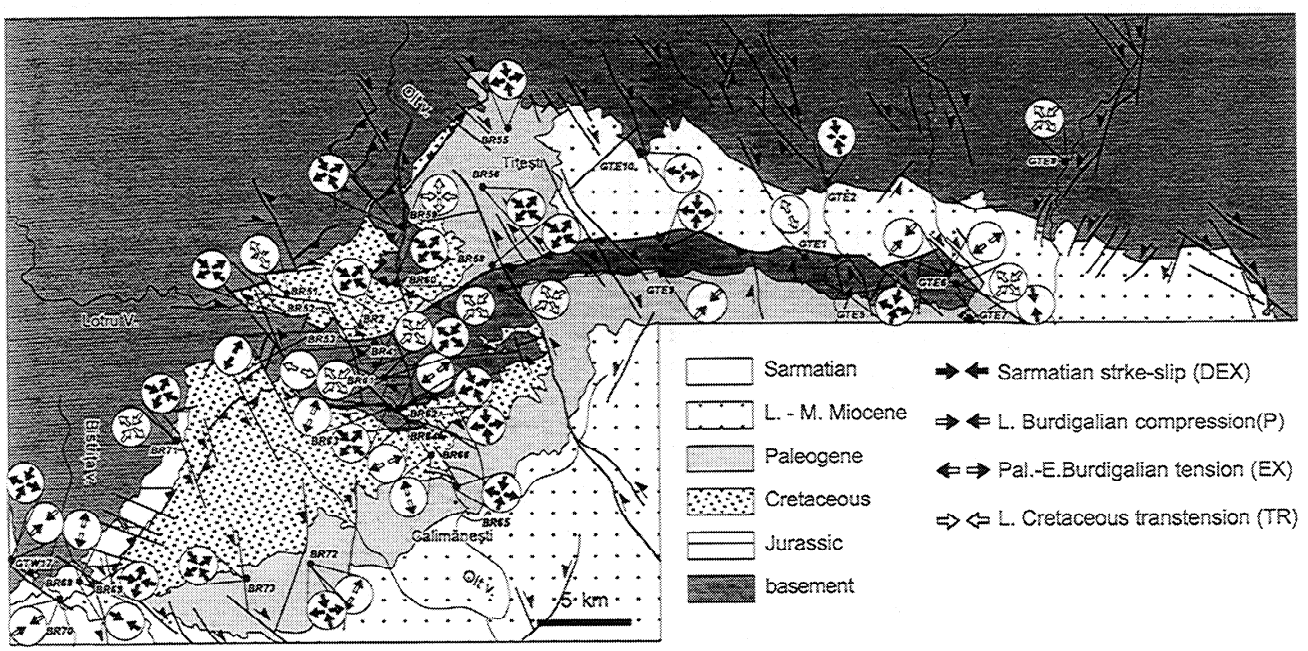

Figure 10. Geological-structural map of the Călimăneşti - Brezoi - Titeşti area with paleostress tensors positions and results. Only the subhorizontal principal axes have been plotted. See Figure 1 for location.

and show a dextral inverse slip component. One such structure is visible south of Racoviţă (west of Titeşti) along the Olt valley where basement units are thrust over Upper Cretaceous sediments, both being covered in the east by uppermost Cretaceous - Paleogene deposits. Previous interpretations [*Szasz*, 1975; *Ştefănescu et al.*, 1986; *Hann*, 1995] considered the basement bodies as nappe slices remnants, generated by the southward advance of the Supra Getic nappe. However, the subvertical position of bounding faults, their opposite vergence at the east and west edges of the block, tension joints geometry, and fault-slip data set analysis in stations BR59 and BR60 rather suggest a positive flower structure interpretation. Younger deformations reactivated this as well as other comparable structures (see section 4.2.2).

4.2.2. N-S to NW-SE tension. The second data set (set "EX" in Table 1) comprises only a relatively small number of measurements and is characterized by pure tensional tensors (Figures 9 to 13). Minimum principal stress axes directions are NNE-SSW (σ_3=195±20°) in the eastern part and 120±20° in the western part of the area, possibly rotated clockwise by later (Sarmatian) deformations. Some scatter is observed in the plots. No age differences can be resolved, and extensional structures are therefore grouped in one set.

No related major structures can be precisely traced at the surface, but this set could be correlated with the extensional features dominating the central and inner portion of the belt [*Neubauer et al.*, 1994] and with the large-scale extensional features observed in the foredeep.

4.2.3. NE-SW compression. The third data set (set "CP" in Table 1) is characterized by pure or oblique compression with a NE-SW oriented maximum compressional axis (σ_1 =240±20°) (Figure 9). The R ratio shows inverse or oblique inverse fault solutions. Related large-scale structures are thrust faults with NNW-SSE orientation, locally reactivated or truncated by later deformations. Most of these structures are located in the western part of the border area, between Jiu and Motru valleys (Figure 12) both in surface and depth structures, in the foredeep (see section 3.). Major surface thrust faults can be interpreted along Sohodol valley (basement and lower Cretaceous deposits were thrust over lower Tertiary sediments) and basement thrusting along Motru valley near Baia de Aramă (near station GTW3, Figure 12).

4.2.4. Strike-slip regime. The fourth data set comprises the largest number of paleostress determinations and was recognized over the entire studied area (Figures 10 to 13). This set is characterized by strike-slip stress tensors and deformation (Figure 9). Two subsets have been defined on the base of the different directions of σ_1 and σ_3 The timing relationships between the two subsets cannot be clearly defined in the field. A single station (GTW18) (see Figure 11), contains fault-slip data from both subsets indicating that the first subset is older, but the low number of faults and the poor quality of the results in this station prevent a final answer on their timing problem. Oblique to subvertical σ_3 directions have been obtained in some instances. In these cases, compressional tensors tend to be associated with the NW vergent backthrust structures commonly found in the areas where the strike of the belt is NE-SW. We associate the tensors with the respective subsets on the basis of the consistent σ_1 directions.

The first subset (marked "DEX1" Table 1) is characterized by a NW-SE compression direction σ_1 =320±15° and a NE-SW tension direction σ_3 = 230±15°. The most common large-scale structures developed during this stage are sets of conjugate strike-slip faults. E-W to WNW-ESE faults are dextral, whereas N-S to NNW-SSE trending faults are sinistral. On the whole, the dextral set of faults seems to dominate. Thrusts also developed during this stage commonly with a NE-SW strike and northwestward vergence.

In the eastern part of the studied area, several structures are identified which we associate with the first subset (Figure 10). The southern margin of the Brezoi-Titeşti Basin is formed by a

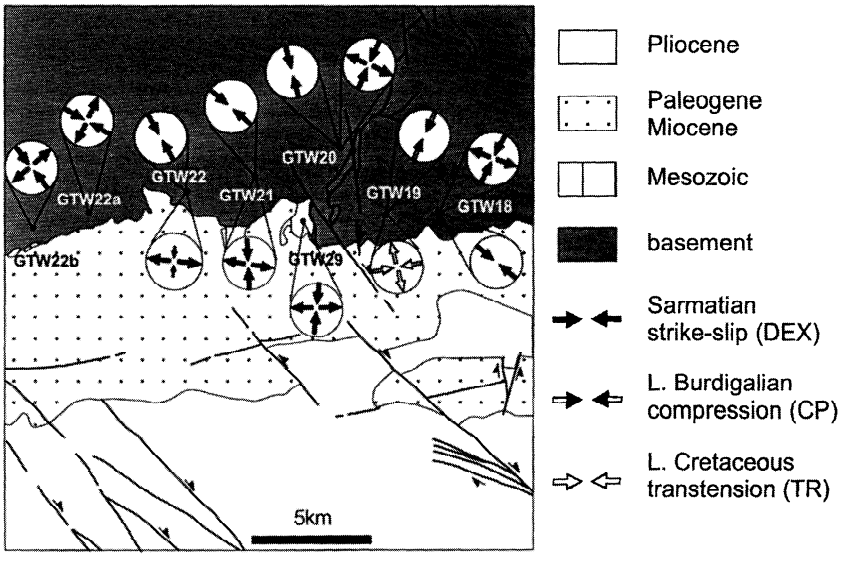

Figure 11. Geological-structural map of the area between Bistriţa and Jiu valleys (central zone) (Figure 1) with paleostress stations positions and results.

E-W trending fault separating the Cozia basement from the overlying Tertiary sediments. The fault possibly formed as a sinistral, normal fault (pre-Alpine shearing in the Cumpăna group [*Iancu and Mărunţiu*, 1994]) but shows a clear inverse-dextral reactivation which we associate with the NW-SE compression. The westernmost termination of the Brezoi-Titeşti Basin is also affected by E-W directed dextral faulting (e.g., stations BR2 and BR52). The Cozia basement south of the same basin is truncated by a large NNW-SSE sinistral fault (near station BR58). A system of N-S to NNW-SSE trending sinistral strike-slip faults of regional importance has been mapped in the area. One of these faults runs along the Olt valley and in the Racoviţa region, displacing the positive flower structure formed during the first deformation event (station BR 59). The flower structure itself is then crossed by E-W trending dextral strike-slip faults. Horsetail structures, with sinistral to normal-sinistral slip, are found on the southern continuation of the described structure along the Olt valley (stations BR61 - BR64). The westernmost part of the area covered by Figure 10 is also strongly deformed with common E-W to WNW-ESE dextral faults. Such structures are found along the Bistriţa valley truncating the Jurassic Vinturariţa Limestone and the thrust along which this is emplaced over younger deposits. Farther to the SE, the western edge of the Călimăneşti Basin is affected by similar dextral faults. In the NW part of the same basin, sinistral NNW-SSE faults cut a backthrust which brings the basement over Upper Cretaceous sediments.

In the Schela-Tismana region (Figure 12), backthrusting along reactivated or newly formed surfaces can be correlated with this set. Such faults are found NE of Motru valley, where Barremian - Aptian limestones are thrust over the Tismana granite, and west of the Sohodol valley, separating Lower Cretaceous limestones from underlying Cenomanian-Senonian clastics. We propose a limited backthrust reactivation of the older (Cretaceous) surface along which the Vălari basement (belonging to the Getic nappe) was thrust over Cretaceous deposits of the Danubian nappe system [*Marinescu et al.*, 1989].

Roughly E-W trending dextral strike-slip faults are common in the westernmost parts of the studied area (Figure 13) where they are among the most important postorogenic structures. Dextral faults segment the Bahna nappe system west of Baia de Aramă [*Berza et al.*, 1994] and the southern part of the Porţile de Fier nappe remnant of the Getic nappe. Less important N-S trending sinistral faults are also found in the area.

The second subset ("DEX2" in Table 1) shows a roughly N-S compression direction, σ_1=175±15°, and E-W tension direction (Figure 9). It can be linked with mainly NNW-SSE to NW-SE trending dextral and subordinate NNE-SSW oriented sinistral strike-slip faults. Purely contractional features, mainly backthrusts, are sometimes observed.

NNW-SSE trending dextral and, less important, NNE-SSW sinistral strike-slip faults are possibly the dominant structural features of the eastern part of the Brezoi-Titeşti Basin where they cut Lower Miocene deposits (Figure 10, near stations GTE1-GTE8) [*Dimitrescu et al.*, 1978, 1985]. Somewhat farther to the east, dextral faults displace the inner basement along the Dâmboviţa valley truncating and tilting the eastern part of the Cozia crystalline.

Dextral NNW-SSE strike-slip faults are very common in the area covered by Figure 11 as, for instance, along Cerna valley segmenting the contact between the Danubian "autochthone" and the Getic nappe.

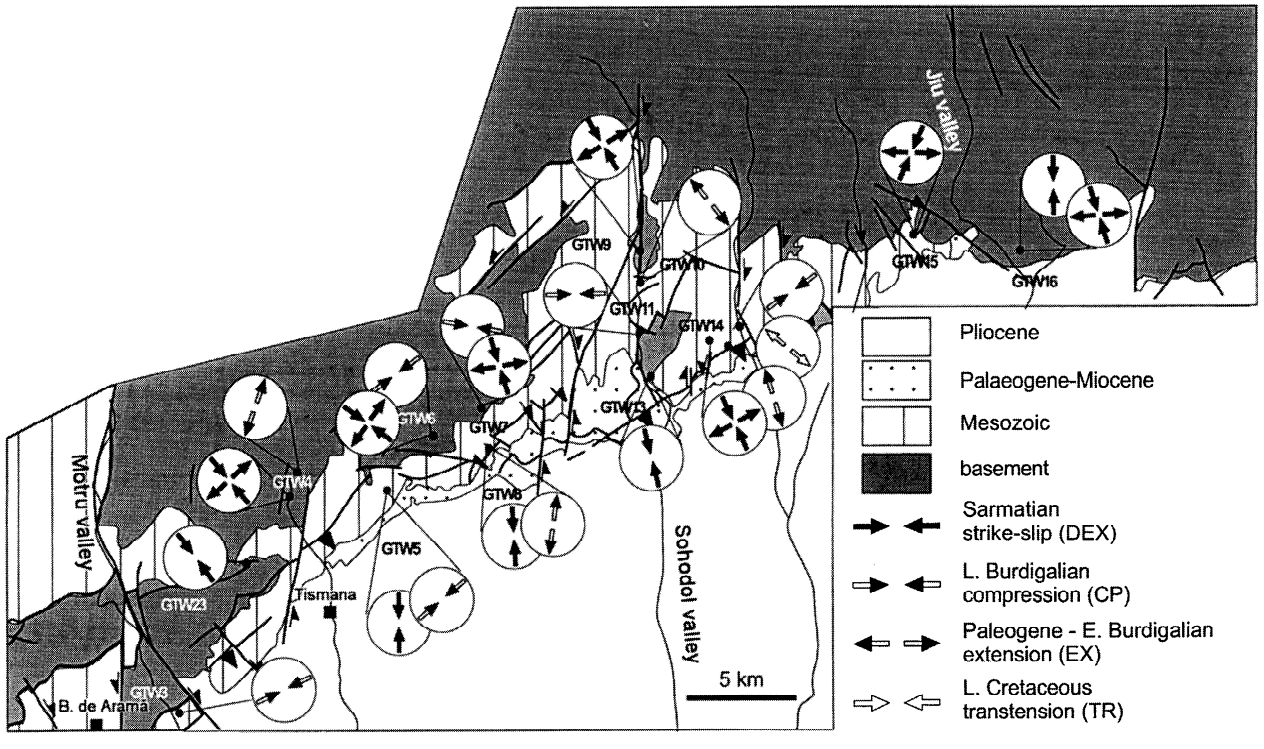

Figure 12. Geological-structural map of the area between Jiu and Motru valleys (central, western zone; Figure 1) with paleostress stations positions and results.

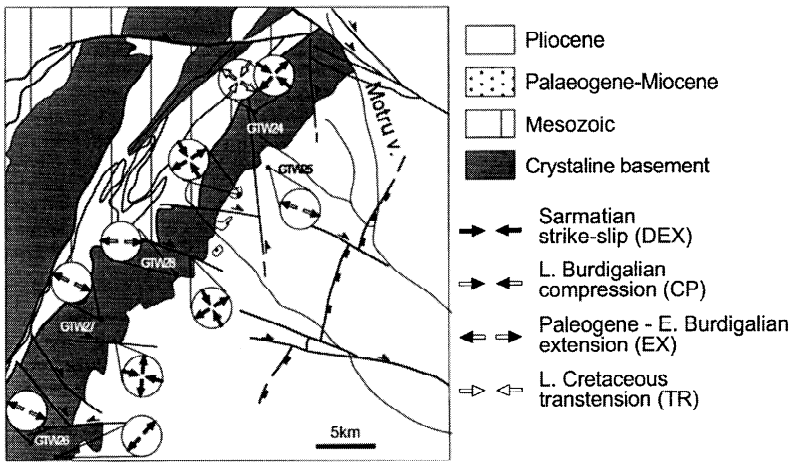

Figure 13. Geological-structural map of the area between Motru and Danube valleys (SW zone; Figure 1) with paleostress stations and results.

Farther to the west (Figure 12), NNE-SSW trending sinistral faults are common. Between Tismana and Schela, they truncate the lower and middle part of Sarmatian deposits and are covered by Upper Sarmatian [*Pop et al.*, 1977; *Savu et al.*, 1984; *Marinescu et al.*, 1989]. A similarly oriented sinistral fault is found along the Sadu valley (east of Bumbeşti Jiu). It has a regional importance because it can be considered as the southern continuation of the sinistral fault forming the eastern limit of the Petroşani Basin [*Berza et al.*, 1994]. Dextral faults are found in the Schela region where they dissect the thrust separating the Schela Jurassic formation from the overlying basement.

5. An Integrated Model for the Tectonic Evolution of the External South Carpathians

5.1. Latest Cretaceous - Early Burdigalian Strike-Slip to Extension

Our data demonstrate that the first structures following the formation of the South Carpathians nappe pile developed under a strike-slip regime characterized by a NE-SW compression and NW-SE tensional axes (data set TR). Mainly transpressional structures formed during this time in the northern parts of the studied area which are sealed by uppermost Cretaceous sediments. The Brezoi-Titeşti Basin opened during this deformation stage possibly controlled by a northward dipping sinistral transtensional fault. At a lager scale, these data suggest an overall sinistral strike-slip regime along a roughly E-W oriented shear corridor.

Strike-slip tectonics were followed, in the studied area, by Paleogene pure extensional deformation (Figure 14a). The timing of the onset of stretching is poorly constrained, but it must have taken place between the Early Paleogene and Early Miocene. Our structural data are somewhat scattered, but they show that tensional axes were NW-SE directed in the western sectors and N-S in the eastern ones ("EX" in Table 1). Normal faults have a NE-SW direction in the west (Figure 2), where they are particularly well developed, and progressively assume a WNW-ESE and E-W trend moving eastward. The amount of stretching seems to decrease in the same direction. Extension controlled lateral changes in thickness and facies of pre-Miocene sediments. The main extensional basin was elongated in a ENE-WSW direction. Basin sediments outcropping east of the Bistriţa (Figure 2) valley are up to 2000 m thick, display southward prograding coarse-grained facies, and show very rapid Eocene subsidence [*Jipa*, 1980, 1982]. The WSW parts of the basin are presently buried under the younger sediments of the Getic Depression, but a correspondence between the basin southern margin and the deep prolongation of the present Pericarpathian line is likely.

Paleogene to Early Burdigalian extension is compatible with the results of flexural modeling along a number of profiles in the Getic Depression [*Maţenco et al.*, 1997]. A strong decrease in effective elastic thickness values from 22 km in the east to 7.5 km in the west has been obtained for the northern Moesian platform loaded by south vergent Carpathians thrusting. The low values in the west spatially coincide with the extensional basin described above.

5.2. Late Burdigalian Contraction

The seismic interpretations we have presented demonstrate that contraction affected the entire area during Late Burdigalian times (Figure 14b). Our structural data (set CP) document NE-SW compression and subvertical σ_3 compatible with the NW-SE directions of thrusts and reverse faults seismically defined in the Getic Depression subsurface.

Late Burdigalian contraction caused the oblique inversion of the older ENE-WSW to E-W oriented extensional basin (Figure 2). In the west, the southern basin margin was inverted and the basin fill uplifted and thrust upon the Moesian platform. Partial inversion of the southern border of the extensional basin occurred also in the east (east of the Olteţ valley) but Late Burdigalian deformation is here mainly confined to the basin fill and is characterized by the formation of small, kilometre-scale piggy-back basins.

5.3. Sarmatian Strike-Slip

Sarmatian deformation took place under a dextral transpressive regime with NW-SE to N-S oriented maximum compression directions (set DEX). Structural observations seem

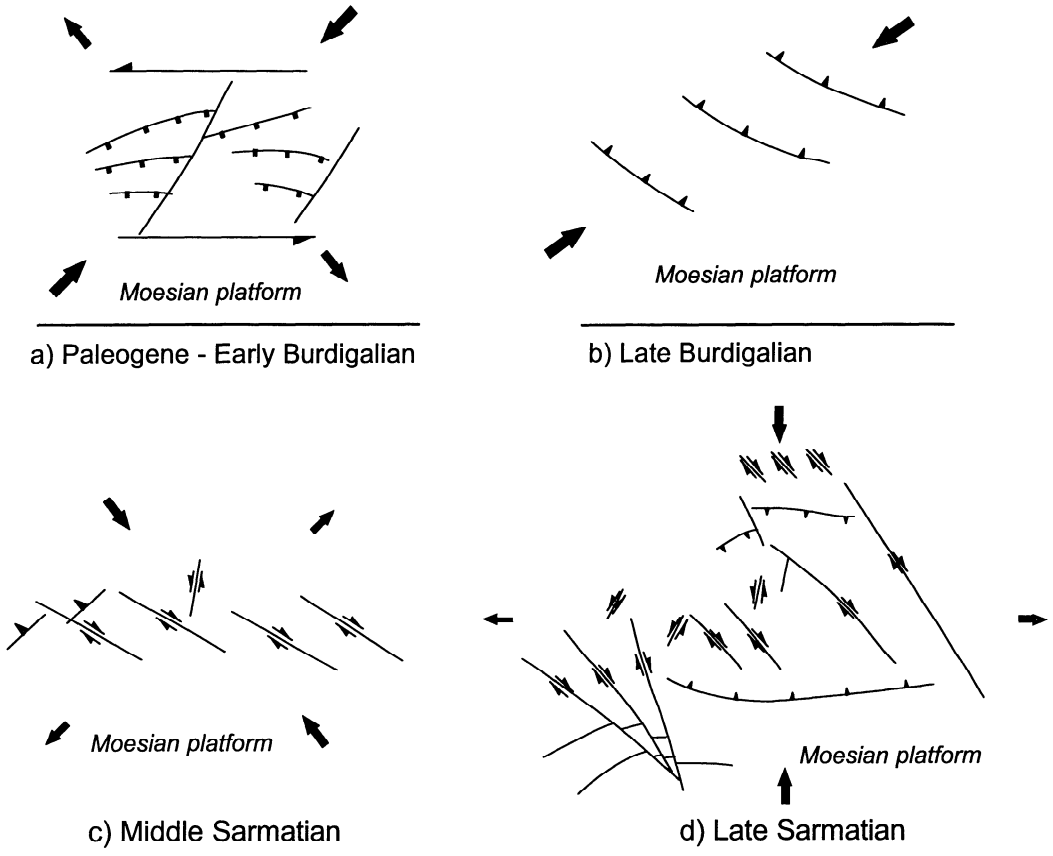

Figure 14. Cartoon showing the main evolutionary stages of the South Carpathians - Moesian platform area during latest Cretaceous to Pliocene. (a) Paleogene - Early Burdigalian transtension - extension; (b) Late Burdigalian contraction; (c) Middle Sarmatian dextral shearing; and (d) Late Sarmatian stress field rotation with dextral transpression, sinistral shearing, and N-S thrusting over Moesian Platform.

to suggest a somewhat younger age for the N-S σ_1 directions. At a larger scale, this is compatible with dextral movements along a roughly E-W trending corridor between the South Carpathians and the Moesian platform (Figures 14c and 14d). Deformation structures associated with this tectonic stage can be recognized over the entire area from the internal regions to the Getic Depression and even in the Moesian platform (Figure 2).

In internal (northerly) areas, NW-SE to N-S contraction caused the dextral transpressional reactivation of the large fault bordering to the south the Brezoi-Titeşti Basin and, possibly slightly later, the formation of NW-SE trending dextral faults mainly observed in the northern part of the same basin. Displacements along these structures can be kinematically related to the Intramoesian fault (Figure 2) (F. *Neubauer,* personal communication, 1995) for which a dextral sense of movement can be established for this time interval [*Tărăpoancă*, 1995]. In this scheme, the northern termination of the Intramoesian fault would form a horsetail system.

In the Getic Depression, the dominant structures associated with this stage are dextral, NW-SE to NNW-SSE trending strike-slip fault zones which can be of crustal importance [e.g., *Maţenco et al.,* 1997] (Figure 2). Sinistral, N-S to NE-SW trending strike-slip faults are also present. They are clearly subordinate to the dextral ones and seem to be slightly younger. Transpressional features, such as typical flower structures, are common along the dextral lineaments and are particularly well visible in seismic sections. Typically, a two-stage evolution can be recognized with a first stage (Middle Sarmatian) when movement was concentrated along one main fault plane followed by a more distributed deformation (Late Sarmatian) associated with the formation of flower structures. This change in deformation style is possibly related to the change in σ_1 direction from NW-SE to N-S. In map view, the uplifts related to the flower structures form at least six lineaments from west to east, Cîlnic, Bâlteni, Bibeşti - Bulbuceni, Ţicleni - Piscu Stejarului, Bustuchini - Romăneşti - Zărneşti, and Stâlpeni - Lăunele, which have an en echelon disposition across the foredeep (Figures 1 and 2). Important oil fields are located along these lineaments.

A dextral crustal fault reaching the sediments of the Moesian platform can be documented in the western part of the Getic Depression and displaces two uplifted basement blocks, (Strehaia and Craiova-Balş-Optaşi uplifts, Figure 2). The areas SW of the fault underwent limited Sarmatian deformation and have remained substantially undeformed ever since. In contrast, deformation in the regions NE of the fault was not only strong during Sarmatian times, but it persisted until Recent times [*Visarion et al.*, 1977]. A zone of low heat flow [*Visarion et al.*, 1985] also follows the fault supporting its crustal importance.

Pure contractional features such as thrusts and reverse faults are common especially in the eastern sectors. Reverse faulting, possibly inverting older normal faults in the northern sectors of

the Paleogene extensional basin, caused the uplift and exposure of the basin fill. In the south, the reactivation of the southern fault margin of the Paleogene to Early Burdigalian extensional basin caused the full development of the frontal thrust which is the largest contractional structure of the area. Burdigalian and older rocks were thrust on the Moesian platform across the frontal thrust.

The total Sarmatian offset across the frontal thrust cannot be determined because of the insufficient information on the geometry of the Moesian Platform beneath the thrust. Shortening in the allochtonous units is > 9% in the west and is >15% in the eastern foredeep [*Morariu et al.*, 1992].

5.4. Late Pliocene Deformations

Small scale reactivations took place in Late Pliocene (Romanian) times, demonstrated by low displacement reverse faults. Most of these faults dip to the south. Subsidence continued mainly in the areas overlying the frontal thrust, particularly in the SE sectors. Up to 1500 m of Pliocene marine to lacustrine sediments were deposited over the thrust system. Meanwhile, strong uplift was taking place in the internal South Carpathians, and Badenian sediments are at elevations of up to 1500 m. The South Carpathians and their foredeep acted as a roughly rigid block tilted toward the south.

6. Regional Correlations and Conclusions

In the preceding sections, we have argued that the tectonic evolution of the frontal area of the South Carpathians can be adequately described in terms of Late Cretaceous to Early Burdigalian transtension to extension, Late Burdigalian contraction and Sarmatian strike-slip. The new data and interpretations we have presented allowed us to provide constraints on regional evolutionary models.

During latest Cretaceous to Paleogene times, the Getic Depression showed clear extensional features which formed WSW-ENE to E-W trending basins. Other sedimentary basins developed during this time in adjacent regions which could be part of the same tectonic stage. We have interpreted the opening of the Brezoi-Titeşti Basin as a consequence of sinistral strike-slip deformation along an E-W trending fault zone. Similarly to what has been observed in more recent case studies [*e.g., Ben-Avraham and Zoback,* 1992], the main faults controlling the opening of the basin formed parallel to the regional strike-slip faults. Another basin which possibly had the same origin is the Bârsei Depression presently situated at the South and East Carpathians junction. Paleogene stretching is contemporaneous with the opening of an extensional basin in the Moldavide domain (East Carpathians) [*Săndulescu,* 1992]. The Late Burdigalian contractional period could be correlated with the Lower Miocene external flysch (Moldavides) deformation in the East Carpathians [*Săndulescu*, 1988].

Deformation during Sarmatian time was characterized by large-scale dextral movements between the Intra-Carpathians and the South Carpathians blocks to the north and the Moesian platform in the south. Dextral strike-slip faults mainly developed in the northern part of the considered area. Local thrusting and backthrusting were mainly concentrated in the NE-SW trending segments of the belt. Large-scale thrusting mainly occurred in the south; its geometry is controlled by the E-W structural grain inherited from previous extension. Small-scale thrusting is contemporaneous with Pliocene N-S contraction in the East Carpathians bending area [*Hyppolite and Săndulescu,* 1996] and with NNE-SSW contraction in the SE part of the Moesian platform [*Bergerat and Pironkov*, 1994].

Plate tectonic models for the Carpathians-Pannonian system generally assume that the Carpathians orogen formed as a consequence of northward and eastward translation of one or more continental blocks (Dacidic and other) and subsequent collision with the Moesian platform in the south and the East European platform in the east and north. According to classic interpretations [*e.g., Săndulescu,* 1984; 1988], Eocene extension affected the East Carpathians and is followed by three stages of contraction during Miocene times. Only the last one would have affected the South Carpathians foredeep. More recent models [*Ratschbacher et al.*, 1993; *Csontos*, 1995; *Linzer*, 1996] rather envisage a more continuous tectonic regime basically characterized by the eastward movement (escape, following the mentioned authors) of the Dacidic blocks presently forming the internal South Carpathians and the substratum of the Transylvania Basin. According to *Ratschbacher et al.* [1993], compression directions changed from W-E to NW-SE during the Miocene and, eventually, to N-S during Pliocene times.

Our reconstructions of latest Cretaceous to Early Burdigalian tectonic regimes are mostly characterized by NW-SE directed tensional and extensional axes and therefore cannot be easily reconciled with these models. This could suggest a decoupling and strain partitioning between the allochthone and the Moesian platform. However, a large degree of freedom is still implicit in these studies, and the need for detailed investigations both at the surface and at depth is emphasized. A similar observation can be made for NE-SW contraction that we have extensively documented for Late Burdigalian times. The last tectonic stages that we have documented are, on the contrary, compatible with overall dextral shearing north of the Moesian platform. However, the total lateral displacements that we were able to document do not exceed a few tens of kilometres.

Acknowledgments. This paper is part of the joint work developed between Tectonics Research Group, VU, Amsterdam and Faculty of Geology and Geophysics, Bucharest University, Romania. The project was sponsored by Shell Romania Exploration B.V., Bucharest and by the Peri-Tethys Program. The help of T. Răbăgia in understanding seismic structures is gratefully acknowledged. Special thanks are addressed to O. Dicea and A. Fülop, Prospectiuni S.A. for useful ideas, helpful comments and continuing support. D. Bondoc and D. Popescu helped in field data collection. M. Ducea and F. Neubauer, are thanked for helpful comments and revisions. The reviews of T. Berza, F. Roure, and M. Ştefănescu helped us in improving the text. This is publication 970125 of the Netherlands School of Sedimentary Geology.

References

Angelier, J., Tectonic analysis of fault slip data sets, *J. Geophys. Res.*, *89*, 5835-5848, 1984.

Angelier, J., From orientation to magnitudes in paleostress determination using fault slip data, *J. Struct. Geol.*, *11*, 37-50, 1989.

Balintoni, I., T. Berza, H. P. Hann, V. Iancu, H. G. Kräutner, and G. Udubaşa, Precambrian metamorphism in the South Carpathians, in *Guide to Excursions*, Problem Comm. IX, Inst. Geol. şi Geofiz., Bucharest, 1989.

Ben-Avraham, Z., and M.D. Zoback, Transform-normal extension and asymmetric basins: An alternative to pull-apart models, *Geology, 20,* 423-460, 1992.

Bergerat, F., and P. Pironkov, Déformations

cassantes et contraintes crétacées à actuelles dans la plate-forme moësienne (Bulgarie), *Bull. Soc. Géol. Fr., 165*, 447-458, 1994.

Berza T., South Carpathians, in *Geological evolution of the Alpine - Carpathian - Pannonian - system*, ALCAPA II, field guidebook edited by T. Berza, *Rom. J. Tect. Reg. Geol., 75*, 37-49, 1994.

Berza, T., H.G. Kraütner, and R. Dimitrescu, Nappe structure of the Danubian window of the central South Carpathians, *An. Inst. Geol. Geofiz., 60*, 31-34, 1983.

Berza, T., V. Iancu, A. Seghedi, I. Nicolae, I. Balintoni, D. Ciulavu, and G. Bertotti, Excursion to South Carpathians, Apuseni mountains and Transylvanian basin: Description of stops, in *Geological Evolution of the Alpine - Carpathian - Pannonian System, ALCAPA II*, field guidebook edited by T. Berza, *Rom. J. Tecton. Reg. Geol., 75*, 105-149, 1994.

Codarcea, A., Vues nouvelles sur la tectonique du Banat et du Plateau du Mehedinţi, *An. Inst. Geol. Rom., XX*, 1-74, 1940.

Csontos, L., Tertiary tectonic evolution of the Intra-Carpathian area: A review, *Acta Volcanol., 7*, 1-13, 1995.

Dicea, O., The structure and hydrocarbon geology of the Romanian East Carpathians border from seismic data, *Petr. Geosci., 1*, 135-143, 1995.

Dimitrescu, R., M. Ştefănescu, A. Rusu, and B. Popescu, Nucşoara-Iezer, geological map Inst. Geol. şi Geofiz., Bucharest scale 1:50.000, sheet 109d, 1978.

Dimitrescu, R., H. P. Hann, I. Gheuca, M. Ştefănescu, L. Szasz, M. Mărunţeanu, E. Şerban, and C. Dumitraşcu, Cumpăna, geological map scale 1:50.000, Inst. Geol. şi Geofiz., Bucharest sheet 109c, 1985.

Hann, H., Central South Carpathians - Petrologic and structural investigations in the area of the Olt Valley, *Rom. J. Tecton. Reg. Geol., 76*, 13-19, 1995.

Hann, H., and L. Szasz, Geological structure of the Olt valley between Câineni and Brezoi (South Carpathians), *D. S. Inst. Geol. Geofiz., 68*, 23-39, 1984.

Hyppolite, J.C., and M. Săndulescu, Paleostress characterization of the "Wallachian" phase in its type area, southeastern Carpathians, Romania, *Tectonophysics, 263*, 235-249, 1996.

Iancu, V., and M. Mărunţiu, Pre-Alpine lithotectonic units and related shear zones in the basement of Getic-Supragetic nappes (South Carpathians), in *Geological Evolution of the Alpine - Carpathian - Pannonian System, ALCAPA II*, field guidebook edited by T. Berza, *Rom. J. Tecton. Reg. Geol., 75*, 87-92, 1994.

Ionescu, N., Exploration History and hydrocarbon prospects in Romania, in *Hydrocarbon of Eastern Central Europe. Habitat, Exploration and Production History*, edited by B. Popescu, pp. 220-250, Springer - Verlag, New York 1994.

Jipa, D., Sedimentological features of the Basal Paleogene in the Vâlsan valley, in *Cretaceous and Tertiary Molasses in the Eastern Carpathains and Getic Depression*, Guidebook Fieldworks Group 3.3, pp. 1-22, Inst. Geol. şi Geofiz., Bucharest, 1980.

Jipa, D., Explanatory notes to the lithotectonic profile of the Getic Paleogene deposits (Southern Carpathians, Romania) (Sedimentological comment to Annex 13), *Veroff. Zentr. Inst. Phys. Erde AdW DDR, 66*, 137-146, 1982.

Jipa, D., Large-scale progradation structures in the Romanian Carpathians: Facts and hypothesis, *An. Inst. Geol. Geof., 64*, 455-463, 1984.

Linzer, H.G., Kinematics of retreating subduction along the Carpathian arc, Romania, *Geology, 24*, 167-170, 1996.

Marinescu, F., G. Pop, N. Stan, and T. Gridan, Peştişani, Geological map Inst. Geol. şi Geofiz., Bucharest scale 1:50.000, sheet 124c, 1989.

Maţenco, L., R. Zoetemeijer, S. Cloetingh, and C. Dinu, Tectonic flexural modeling of the Romanian Carpathians foreland system, *Tectonophysiscs*, 1997.

Morariu, D., L. Maţenco, and C. Dinu, Structural styles of contact zone between Southern Carpathians Foredeep and Moesian Platform, in, Geological evolution of the internal Eastern Alps, Carpathians and of the Pannonian Basin, *Terra Nova Abstr., 4*, 46, 1992.

Motaş, C., Nouvelles donnés sur les rapports structuraux entre les Carpathes Méridionales et la depression gétique, *An. Ist. Geol. Geofiz, 60*, 141-146, 1983.

Murgoci, G. M., Contributions a la tectonique des Karpathes Meridionales, *C. R. Acad. Sci. Paris, 9*, 4-20, 1905.

Murgoci, G.M., The geological synthesis of the South Carpathians, *C. R. XI Congr. Geol. Int.*, 871-881, 1912.

Neubauer, F., H. Fritz, E. Wallbrecher, and A. V. Bojar, Paleostress patterns in the Southern Carpathians: Strike-slip and extension by oroclinal bending, in *Geological evolution of the Alpine - Carpathian - Pannonian System, ALCAPA II*, edited by T. Berza, *Rom. J. Tecton. Reg. Geol., 75*, 39-40, 1994.

Pop, G., T. Berza, F. Marinescu, I. Stănoiu, and I. Hîrtopanu, Tismana, Geological map scale 1:50000, Inst. Geol. şi Geofiz. Bucharest, sheet 123d, 1977.

Răbăgia, T., and A. Fülop, Sintectonic sedimentation history in the Southern Carpathians Foredeep, in *Geological evolution of the Alpine - Carpathian - Pannonian System, ALCAPA II*, field guidebook edited by T. Berza, *Rom. J. Tecton. Reg. Geol., 75*, 48, 1994.

Ratschbacher, L., H. G. Linzer, F. Moser, R. O. Strusievicz, H. Bedelean, N. Har, and P. A. Mogoş, Cretaceous to Miocene thrusting and wrenching along the central South Carpathians due to a corner effect during collision and orocline formation, *Tectonics, 12*, 855-873, 1993.

Royden, L.H., Late Cenozoic Tectonics of the Pannonian Basin System, in *The Pannonian Basin, a Study in Basin Evolution*, edited by L. H. Royden and F. Horvath, *AAPG Mem., 45*, 27-48, 1988.

Săndulescu, M., Geotectonica României, Ed. Tehnică, Bucharest, 1984.

Săndulescu, M., Cenozoic Tectonic History of the Carpathians, in *The Pannonian Basin, a Study in Basin Evolution*, edited by L. H. Royden and F. Horvath, *AAPG Mem., 45*, 17-25, 1988.

Săndulescu M., Réunion extraordinaire de la Société Géologique de France en Roumanie, *Guide des Excursions*, Inst. Geol. şi Geofiz., Bucharest, 1992.

Savu, H., N. Stan, S. Năstăseanu, F. Marinescu, and I. Stănoiu, Schela, Geological map 1:50000 Inst. Geol. şi Geofiz. Bucharest, sheet 124b, 1984.

Ştefănescu, M., and P. Polonic, Deep structure in Romania and the related hydrocarbon prospects, *First Break*, 2, 99-105, 1993.

Ştefănescu, M., L. Szasz, E. Bratu, M. Ştefănescu, A. Rusu, and A. M. Piliuţă, Geology of the Titeşti Depression, *Dări seamă şedinţelor, 70*, 133-146, 1986.

Ştefănescu, M., and 20 others, Geological cross sections no. B 1-7, scalc 1:200,000, Inst. Geol. şi Geofiz., Bucharest, 1988.

Streckeisen, A., Sur la tectonique des Carpathes Méridionales, *An. Inst. Géol., 16*, 327-481, 1934.

Szasz, L., Biostratigrafia şi paleontologia Cretacicului superior din bazinul Brezoi, *Dări seamă şedinţelor*, 62, 189-220, 1975.

Tărăpoancă, M., Tectonica faliei Intramoesice (Tectonics of the Intramoesian Fault), Master thesis, Univ. Bucharest, 1995.

Visarion, M., M. Săndulescu, I. Dragonescu, M. Drăghici, I. Cornea, and M. Popescu, România. Map of recent crustal vertical movements, Inst. Geol. şi Geofiz., Bucharest, Romania, 1977.

Visarion, M., A. Butac, and C. Georgescu, Romania geothermal map, Inst. Geol. şi Geofiz., Bucharest, Romania, 1985.

G. Bertotti and S. Cloetingh, Faculty of Earth Sciences, Vrije Universiteit, De Boelelaan 1085, 1081 HV Amsterdam, Netherlands. (e-mail: bert@geo.vu.nl)

C. Dinu and L. Maţenco, Faculty of Geology and Geophysics, University of Bucharest, 6 Tr. Vuia str., section 1, 70139 Bucharest, Romania. (matl@ter1.sbnet.ro)

(Received July 26, 1996;
revised February 21, 1997;
accepted April 1, 1997.)